J. Fluid Mech. (2010), *vol.* 642, *pp.* 147–157.
doi:10.1017/S0022112009992424

Super free fall

E. VILLERMAUX[1]† AND Y. POMEAU[2]

[1]Aix-Marseille Université, IRPHE, 13384 Marseille Cedex 13, France

[2]Department of Mathematics, The University of Arizona, 617 N. Santa Rita Avenue, PO Box 210089 Tucson, AZ 85721-0089, USA

(Received 29 July 2009; revised 17 September 2009; accepted 17 September 2009)

The free fall of a liquid mass through vertical tubes with a weakly increasing cross-section induces an acceleration of the upper liquid interface larger than gravity. The phenomenon is well described by a one-dimensional inviscid model. The super acceleration of the upper interface comes from the additional positive pressure gradient caused by the expanding geometry, which adds to the gravity body force. A perturbative expansion of this base solution further accounts for the interface shape and stability. In particular, the positive pressure gradient at the interface makes it unstable, forming a concentrated 'nipple' on top of the essentially flat base solution. We discuss the possible connexion of these findings with the problem of wave breaking in free surface flows.

Key words: free surface flows, stability Rayleigh–Taylor instability, tubes superacceleration

1. Introduction

Can an object, solely moved by gravity forces, fall faster than gravity ? The quick answer might be no, but a detailed analysis shows that the correct answer is obviously yes. In a conservative system, if the available energy happens to be concentrated in an ever smaller fraction of the initial system mass, it will accelerate with no bound. This is, for instance, the case of the celebrated falling chain problem (Calkin & March 1989; Schager, Steindl & Troger 1997) where the downward acceleration of the released tip of a folded chain hanging in gravity diverges at the end of the fall.

Spontaneous super accelerations (i.e. larger that g) in fluids moved by gravity do not seem to have been explored in a systematic way, including experimentally, with the notable exception of Penney & Price (1952). These authors studied the shape and dynamics of a two-dimensional standing gravity wave, and found that above a critical wave steepness, the crest height becomes pointed, and is expected to fall faster than g, a situation they called 'physically untenable'. Taylor (1953) experimentally confirmed some of their predictions, and noticed a strong instability at the moment the crest became a sharp ridge, rapidly assuming a three-dimensional character. Accelerations larger than g have been found to possibly occur in some special circumstances with suitably conjectured velocity potentials (Clavin & Williams 2005; Duchemin 2008). Here, thanks to a specially designed experiment we show that super accelerations do occur as a result of coupling between inertia and appropriate confining geometry.

† Also at: Institut Universitaire de France. Email address for correspondence: villerma@irphe.univ-mrs.fr

	$\tan(\alpha)$	$R(0)$ (cm)	$\beta = 1 - R(h(0))/R(0)$
Tube 1	0.03	3.3	0.33
Tube 2	0.07	3.7	0.52

TABLE 1. Geometry of the two transparent glass tubes used in the experiments.

Fluids moving in tubes have a long history in fluid and wave mechanics, starting with Newton (1687), who derived the period of oscillation of a fluid mass in a U tube, and used the result to infer the celerity of gravity waves at the surface of a liquid. The acceleration never exceeds g in a two-armed tube (Bernoulli 1738), while it may do so in a three-armed tube (Hirata & Craik 2003). The reason is that the liquid falling in a given arm has twice as much space to empty in a three-armed tube, and thus falls faster. The principle of our experiment exploits this effect in a continuous manner, as we are considering a single tube with a gradually increasing cross-section.

Section 2 describes the experimental set-up used to produce downward motion accelerating faster than gravity, and our accompanying observations. Section 3 analyses the free fall of a liquid mass through tubes with varying cross-section, and more specifically in those with an ever increasing space offered in the direction of the motion, namely weakly divergent conical tubes. Section 4 analyses the shape of the liquid upper interface as induced both by the structure of the base flow and by its super acceleration. The interface develops a positive weak curvature and a strong localized negative one, in the form of a 'nipple', signature of an inertial instability. Section 5 discusses the possible relevance of these findings to the problem of wave breaking in free surface flows.

2. Experimental set-up and observations

The idea of our device is a simple one: consider a uniform column of fluid in free fall inside a vertical rigid cylindrical tube. In the absence of viscosity, its acceleration is exactly g. Suppose now that the tube has a non-constant cross-section. Let this cross-section be piecewise constant, equal to a_b in the lower part of the tube and to another constant $a_u \ll a_b$ in the upper part. After the tube is filled with an incompressible, inviscid and wetting liquid, we open abruptly to the atmosphere its bottom end where the cross-section is the largest, the upper end remaining always open. Because $a_u \ll a_b$, the acceleration will be dominated by the one of the largest mass of fluid, the one filling the lower part of the tube. The fluid will be there in free fall, with a downward acceleration close to g. By mass conservation, enforced by the wetting condition (the liquid is forced to stick to the tube wall), the downward acceleration of the fluid in the top tube will be $g\,(a_b/a_u)$, larger than g. Experimentally, however, this idea cannot be realized so simply. Real fluids are viscous and a discontinuity of cross-section is a major source of dissipation at non-negligible Reynolds number. Practically the multiplying factor generated by a sudden increase of cross-section is overbalanced by the dissipation near the discontinuity. We have therefore chosen a smoothly expanding tube, with a rate of expansion less than about 10 %. A larger expansion rate increases dramatically the growth and detachment of the viscous boundary layers along the tube walls, and make the phenomenon disappear in practice.

We use two different liquids, water (mass density $\rho = 10^3\,\mathrm{kg\,m^{-3}}$, surface tension $\gamma = 70 \times 10^{-3}\,\mathrm{N\,m^{-1}}$, viscosity $\nu = 10^{-6}\,\mathrm{m^2\,s^{-1}}$) and ethanol (mass density $\rho = 810\,\mathrm{kg\,m^{-3}}$, surface tension $\gamma = 22 \times 10^{-3}\,\mathrm{N\,m^{-1}}$, viscosity $\nu = 1.52 \times 10^{-6}\,\mathrm{m^2\,s^{-1}}$) and two glass tubes. A conical tube is characterized by its opening angle α, the radius at its bottom

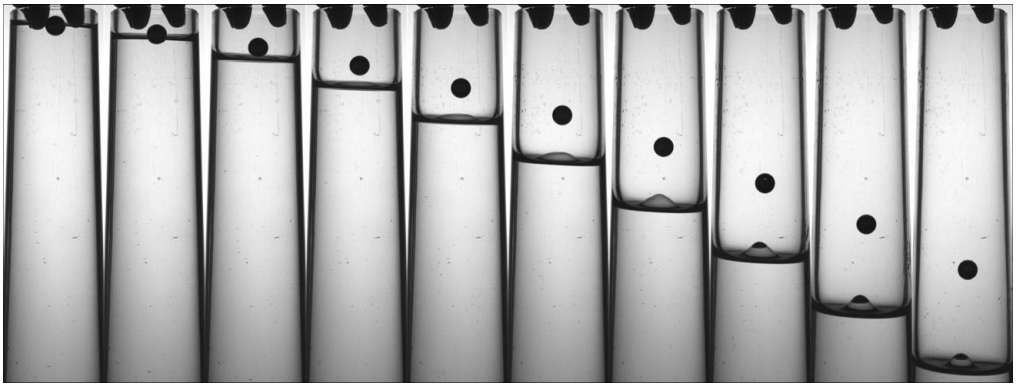

FIGURE 1. Free fall of a steel ball, and comparison with the position of the liquid interface in Tube 1, with ethanol. The pictures are equally spaced in time.

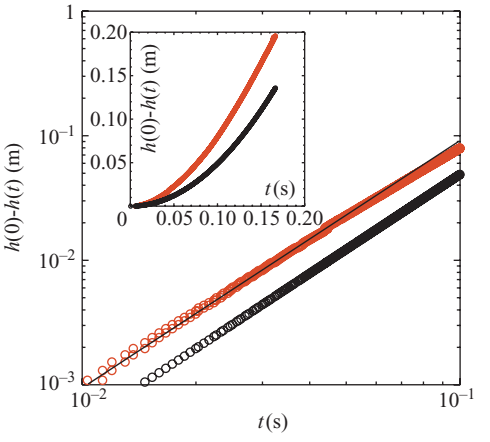

FIGURE 2. The trajectory of the upper interface (○), and that of the steel ball (○) in the experiment shown in figure 1, using Tube 1. The insert is in linear units. While the trajectory of the steel ball is ruled by $\ddot{h}(t) = -g$ with $g = 9.81\,\mathrm{m\,s^{-2}}$, the line on top of the interface trajectory is $\ddot{h}(t) = -g/(1-\beta)$ with $\beta = 0.33$ (see table 1).

$R(0)$ and by the ratio of its bottom radius to that at the liquid initial filling height $R(h(0))$ detailed in table 1 (see also figure 3).

The experiment consists in opening abruptly the lower end of a tube filled before with liquid. As seen in figure 1, the emptying time of the tube is shorter than that expected from pure gravity: the comparison with the free fall of an isolated heavy steel ball released afterwards, and superimposed with the liquid trajectory shows that the liquid upper interface always precedes the ball. The ball trajectory exhibits the characteristic parabola, while that of the liquid interface seems to do so as well, but with an apparent larger curvature (figure 2), sign of a super acceleration.

Also visible on the instantaneous pictures of the liquid interface is its curvature, building up as time proceeds. There is a weak positive hollow curvature developing slowly on top of which a strong localized negative curvature grows in the form of a concentrated 'nipple'. The following intends to describe these phenomena.

3. Free fall with varying cross-section

Guided by our observations, the dynamical equations we start from are for the vertical component $w(r, z, t)$ and radial component $u(r, z, t)$ of the fluid velocity in

cylindrical coordinates, with no azimuthal dependence. The position variables are the vertical coordinate z (pointing upwards) and the radius r. The fluid equations for w and u read, with p the pressure, ρ the fluid density and g the gravity acceleration pointing downwards

$$\partial_t w + w\partial_z w + u\partial_r w = -\partial_z p/\rho - g, \tag{3.1}$$

$$\partial_t u + w\partial_z u + u\partial_r u = -\partial_r p/\rho, \tag{3.2}$$

$$r\,\partial_z w + \partial_r(ru) = 0. \tag{3.3}$$

Viscosity can be neglected: for emptying times of the order of $t = 0.1$ s, the typical thickness of the viscous boundary layer $\sqrt{\nu t}$ is a fraction of a millimetre, much less than the tube radii, in the centimetre range. Because the cross-section changes slowly as a function of the vertical distance, we use a slender slope approximation. At leading order we consider the dynamics of the vertical velocity averaged over the cross-section of area $a(z) = \pi R^2(z)$:

$$w(z,t) = \frac{2}{R^2(z)} \int_0^{R(z)} r\, w(r,z,t)\, \mathrm{d}r, \tag{3.4}$$

which from (3.3) and the kinematic condition at the tube wall $\mathrm{d}R/\mathrm{d}t = \partial_t R + w(R,z,t)\,\partial_z R$ provides

$$\partial_t R^2 + \partial_z(w(z,t)\,R^2) = 0. \tag{3.5}$$

The tube being rigid, and its radius $R(z)$ independent of time, we find from (3.5) that the time dependent vertical flux

$$j(t) = a(z)\,w(z,t) \tag{3.6}$$

is constant along z.

3.1. *Base state*

At leading order in the slender slope limit, the Euler equations yield an equation for $w(z,t)$ which writes, together with its boundary conditions at the opened tube ends in $z = 0$ and at the upper interface in $z = h(t)$,

$$\partial_t w + w\partial_z w = -\partial_z p/\rho - g \quad \text{with} \quad p(0) = p(h(t)) = 0, \tag{3.7}$$

$$\partial_z(a(z)\,w) = 0. \tag{3.8}$$

We neglect at this stage the pressure due to the curvature of the interface; this will be discussed in § 4. Denoting $\mathrm{d}h(t)/\mathrm{d}t = \dot{h}$ and from the constancy of the flux $j(t)$, one has

$$w(z,t) = \frac{a(h)}{a(z)}\,\dot{h}. \tag{3.9}$$

Inserting the above expression for $w(z,t)$ into (3.7) leads to

$$\frac{a(h)}{a(z)}\,\ddot{h} - \frac{a^2(h)\,\partial_z a}{a^3(z)}\,(\dot{h})^2 = -\frac{1}{\rho}\partial_z p - g. \tag{3.10}$$

Upon integration between $z = 0$ and $z = h(t)$ and with the zero pressure condition at these boundaries, (3.10) yields the classical solution (Paterson 1983):

$$\left(a(h)\int_0^h \frac{\mathrm{d}z}{a(z)}\right)\ddot{h} + \frac{1}{2}\left(1 - \frac{a(h)^2}{a(0)^2}\right)(\dot{h})^2 = -g\,h. \tag{3.11}$$

This yields back free fall for $a(z)=a(0)$ constant. Starting from rest ($\dot{h}(t=0)=0$), (3.11) predicts that the initial acceleration of the interface will be

$$\ddot{h} = -g \frac{h}{a(h)\displaystyle\int_0^h \frac{\mathrm{d}z}{a(z)}}. \tag{3.12}$$

This acceleration is larger (in absolute value) than the acceleration of gravity provided

$$\frac{h}{a(h)} > \int_0^h \frac{\mathrm{d}z}{a(z)}, \tag{3.13}$$

a condition fulfilled when the cross-section area $a(z)$ decreases at higher elevation. The origin of this super acceleration is readily understood from the structure of the pressure field induced by the fluid motion. Inserting the early time dynamics of (3.12) into (3.10), one sees that the early time pressure gradient reads

$$\frac{\partial_z p}{\rho g} = \frac{h}{a(z)\displaystyle\int_0^h \frac{\mathrm{d}z}{a(z)}} - 1. \tag{3.14}$$

When condition (3.13) is fulfilled, that is when the upper interface super accelerates, the pressure gradient at the interface in $z=h(t)$ is *positive*, demonstrating that the fluid is 'sucked' downwards, with a pressure force adding to the pure gravitational body force. Conversely, the fluid is slowed down at the bottom interface where, as can be seen from (3.14), $\partial_z p$ is negative. For an area $a(z)$ decaying smoothly with z, the pressure $p(z,t)$ is everywhere negative. The falling motion is thus accompanied by rearrangements of the fluid particles within the confining volume which they are enforced to fill by the adherence condition. As expected, the consequence is a slower motion in the large section area of the volume, and a faster one in the small region close to the upper surface.

A natural question to ask is about the motion of the fluid *centre of mass*, that is the mass weighted velocity $\langle w\rangle$ of the fluid mass m enclosed within the volume Ω

$$\langle w\rangle = \frac{1}{m}\int_\Omega \rho\, w\, \mathrm{d}\Omega = \frac{\displaystyle\int_0^h w(z,t)\, a(z)\, \mathrm{d}z}{\displaystyle\int_0^h a(z)\, \mathrm{d}z}, \tag{3.15}$$

which, since the flux $j(t)=a(h)\dot{h}=a(z)w(z,t)$ is constant along z, writes

$$\langle w\rangle = \frac{a(h)\dot{h}\, h}{\displaystyle\int_0^h a(z)\, \mathrm{d}z}. \tag{3.16}$$

Making use of (3.12), the early time acceleration of the centre of mass is thus

$$\partial_t\langle w\rangle = -g \frac{h^2}{\displaystyle\int_0^h a(z)\, \mathrm{d}z \int_0^h \frac{\mathrm{d}z}{a(z)}}. \tag{3.17}$$

The Cauchy–Schwarz inequality states that, for any two real functions $f(z)$ and $g(z)$, one has $|\int f(z)g(z)\mathrm{d}z|^2 \leqslant \int |f(z)|^2\mathrm{d}z \cdot \int |g(z)|^2\mathrm{d}z$; setting $f(z)=\sqrt{a(z)}$ and $g(z)=1/\sqrt{a(z)}$ leads, from (3.17), to $|\partial_t\langle w\rangle| \leqslant g$. The fall of the centre of mass is

initially slower than gravity, whatever $a(z)$ may be (i.e. increasing of decreasing with z). The super acceleration of the upper interface in (3.12) is then all the more remarkable.

3.2. *The case of conical tubes*

For a conical tube with constant opening angle α as those used in the present experiments with radius $R(z) = R(0) - z\tan\alpha$, one has

$$a(z) = a(0)(1 - \beta z/h(0))^2 \quad \text{with} \quad a(0) = \pi R^2(0), \tag{3.18}$$

where

$$\beta = \frac{h(0)}{R(0)}\tan\alpha = 1 - \frac{R(h(0))}{R(0)}, \tag{3.19}$$

with $h(0)$ the height filled with liquid at $t = 0$ in the tube. Since the tube is thinner at the top, $0 < \beta < 1$. From (3.12) and (3.14), one has in that case

$$\ddot{h}\big|_{t=0} = -\frac{g}{1-\beta} \quad \text{and} \quad \left.\frac{\partial_z p}{\rho g}\right|_{z=h(0)} = \frac{\beta}{1-\beta} > 0. \tag{3.20}$$

For the tubes in table 1, the early time acceleration can thus be appreciably larger than gravity. This is quantitatively confirmed by measurements of the upper interface (mean) kinematics, as seen in figure 2 showing that the initial trajectory is not only of a pure gravitational type (i.e. $\ddot{h} = -g'$), but that the apparent acceleration g' is indeed that anticipated from (3.20). The neglected nonlinear term in (3.11) increases the super acceleration at late stages; the observed slowdown is probably attributable to the friction of the engulfed air at the upper tube opening, which we do not account for.

4. Shape of the interface

4.1. *A pure kinematic effect*

We return to the complete set of equations and wonder what the first correction to the plug-flow solution we have derived above will be (this is the first term beyond the leading order in the slender slope limit). We want to know the consequence on the liquid interface shape of the radial flow induced by the slow cross-section opening. The velocity and pressure fields now incorporate first-order corrections as

$$w(r, z, t) = w(z, t) + w^{(1)}(r, z, t), \tag{4.1}$$

$$u(r, z, t) = 0 + u^{(1)}(r, z, t), \tag{4.2}$$

$$p(r, z, t) = p(z, t) + p^{(1)}(r, z, t), \tag{4.3}$$

where $w(z, t) = j(t)/\pi R^2(z)$ are the axial velocity and $p(z, t)$ the pressure computed before. Inserting (4.1) and (4.2) into the incompressibility condition (3.3) leads, at dominant order, to

$$u^{(1)}(r, z, t) = -\frac{r}{2}\partial_z w(z, t) = r\,\frac{j(t)\partial_z R}{\pi R^3}, \tag{4.4}$$

which, inserted into (3.2) provides the correction for the pressure

$$-\frac{p^{(1)}}{\rho} = \frac{r^2}{2}\frac{\partial_t j(t)\partial_z R}{\pi R^3} + C(z, t), \tag{4.5}$$

at initial time when $j(0) = 0$. That pressure is defined up to a constant $C(z, t)$ that we take as zero. Now, from that pressure and (3.1), we get the correction to the vertical

motion as

$$w^{(1)}(r,z,t) = -\frac{3}{2} r^2 \frac{\partial_t j(t) (\partial_z R)^2}{\pi R^4}. \tag{4.6}$$

The two velocities $u^{(1)}$ and $w^{(1)}$ allow to compute the kinematics of the liquid upper interface solely due to these subdominant contributions to the flow field. Indeed, calling $h(r,t) = h(t) + Z(r,t)$ the vertical location of the interface, its motion obeys

$$\frac{\mathrm{d}h}{\mathrm{d}t} = \frac{\partial h}{\partial t} + u \frac{\partial h}{\partial r}. \tag{4.7}$$

For the interface shape $Z(r,t)$ superimposed on top of the trivial plug displacement $\dot{h}(t) = w(h,t)$ computed before, this yields,

$$\partial_t Z = w^{(1)} - u^{(1)} \partial_r Z. \tag{4.8}$$

Or, making use of (4.4) and (4.6)

$$\partial_t Z = -\frac{j(t)}{\pi R^2} \frac{\partial_z R}{R} \left(\frac{3}{2} \frac{\partial_z R}{R} r^2 + r \partial_r Z \right). \tag{4.9}$$

Introducing the interface curvature $\kappa(t) = 1/\mathscr{R}_+(t)$ such that $Z(r,t) = \kappa(t) r^2/2$ where $\mathscr{R}_+(t)$ is the interface radius of curvature, and remembering that $j(t) = \pi R^2 \dot{h}$ leads to

$$\partial_t \kappa(t) = -\dot{h} \frac{\partial_z R}{R} \left(3 \frac{\partial_z R}{R} + 2\kappa(t) \right). \tag{4.10}$$

The interface curvature first increases ($\dot{h} < 0$), and then saturates ($\partial_z R < 0$). The early time dynamics, with $\dot{h} = -g't$ and g' the effective mean acceleration of the interface computed in § 3 is thus expected to be

$$\kappa(t) = \frac{3}{2} \left(\frac{\partial_z R}{R} \right)^2 g' t^2 \tag{4.11}$$

or, for the conical tubes described in § 3.2 for which $g' = g/(1-\beta)$ and $\partial_z R = -\tan\alpha$

$$\kappa(t) = \frac{3}{2} \frac{g}{1-\beta} \frac{(\tan\alpha)^2}{R^2(h(0))} t^2. \tag{4.12}$$

The above relationship is in quantitative agreement with the measurements reported in figure 3.

4.2. *The central nipple: Rayleigh–Taylor instability*

We now turn to a spectacular feature of the super free fall phenomenon, the formation of a central 'nipple'. If the slow opening of the streamlines induce a weak positive curvature of the interface, a strong effect accompanying the fall of the liquid volume is the onset of a positive pressure gradient at the upper interface (see (3.14) and (3.20)). This interface is also a density interface since it separates a dense liquid phase from an essentially evanescent medium at atmospheric pressure. The base state of the flow, as computed in §§ 3 and 4.1, is thus potentially Rayleigh–Taylor unstable.

Introducing the perturbed quantities $u^{(2)}(r,z,t)$, $w^{(2)}(r,z,t)$ and $p^{(2)}(r,z,t)$ on top of those already introduced in (4.1)–(4.3), and accounting for the liquid incompressibility (3.3) leads the classical harmonicity condition for the pressure $\nabla^2 p^{(2)} = 0$. For an interface position writing now $h(r,t) = h(t) + Z(r,t) + \xi(r,t)$ with

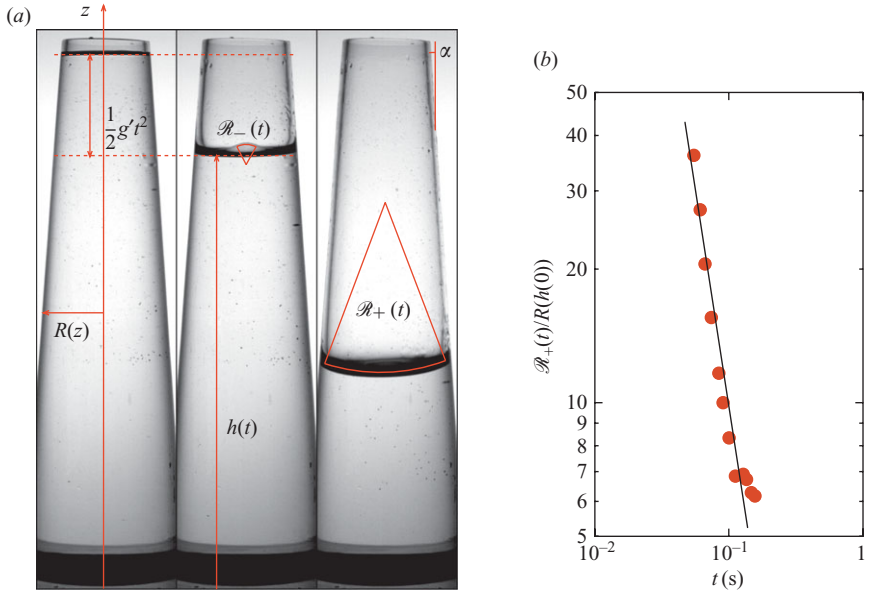

FIGURE 3. (*a*) Definition of the cone geometry, and of the various quantities of interest. (*b*) Evolution of the positive curvature of the upper interface for Tube 2 and $R(h(0)) = 1.8$ cm. The line is (4.12) with $\kappa(t) = 1/\mathscr{R}_+(t)$.

$\xi(r, t) \sim \sum_k J_0(k\,r)\,\mathrm{e}^{-\mathrm{i}\omega t}$ a family of axisymmetric perturbations, one has

$$p^{(2)}(r, z, t) = \sum_k \tilde{p}(k) J_0(k\,r)\,\mathrm{e}^{k(z-h)-\mathrm{i}\omega t}. \tag{4.13}$$

Denoting γ the liquid surface tension, the (linearized) boundary condition for the pressure at the interface is $p^{(2)}(r, h, t) = (\partial_z p)\,\xi - \gamma\nabla^2\xi$, thus leading, together with the kinematics condition $w^{(2)}(r, h, t) = \partial_t\xi$ and vertical momentum equation $\rho\,\partial_t w^{(2)} = -\partial_z p^{(2)}$ around $w(z, 0) = 0$, to the dispersion relation

$$\rho\,\omega^2 = -\partial_z p\,k + \gamma\,k^3. \tag{4.14}$$

As expected, when the pressure gradient is positive at the interface, instability occurs. In the conical tube geometry, that dispersion relation reads (see (3.20))

$$\omega^2 = -\frac{\beta}{1-\beta}\,g\,k + \frac{\gamma}{\rho}\,k^3, \tag{4.15}$$

where the destabilizing term is trivially interpreted as the effective body force $g - g' = g - g/(1-\beta) = -g\beta/(1-\beta)$ pointing upwards in the reference frame of the liquid. The cutoff of this instability is at the usual capillary wavenumber k_c and the most amplified wavenumber is $k_m = k_c/\sqrt{3}$ with growth rate σ, which we write including the pre-factors

$$k_c = \sqrt{\frac{\beta}{1-\beta}\frac{\rho g}{\gamma}} \quad \text{and} \quad \sigma = \sqrt{\frac{2}{3\sqrt{3}}}\sqrt{\frac{\beta}{1-\beta}\,g\,k_c}. \tag{4.16}$$

The corresponding wavelength $\lambda = 2\pi/k_m$ is in practice of the order of the tube radius $R(h(0))$, as experiments show (see figure 1), and much smaller than the weak positive curvature $\mathscr{R}_+$ described in § 4.1. This instability gives birth to the central nipple visible

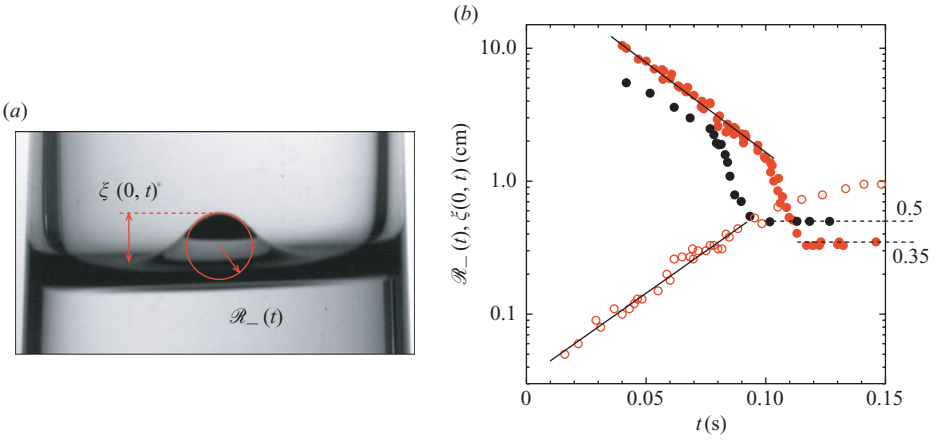

FIGURE 4. (*a*) Definition of the nipple radius of curvature $\mathscr{R}_-(t)$ and of its amplitude $\xi(0,t)$. (*b*) Amplitude (○) and nipple radius of curvature (●) for Tube 1 with ethanol as working liquid. Same with water as working liquid (●). The lines haves slopes $\pm\sigma = \pm\, 27\,\mathrm{s}^{-1}$ according to (4.16). The saturated values of the nipple radius of curvature $\mathscr{R}_-$ are 3.5 mm for ethanol and 5 mm for water, in quantitative agreement with (4.18).

in the experiments, pointing upwards like a dripping drop hangs downwards at a faucet orifice. Because of the instability development, the radius of curvature $\mathscr{R}_-(t)$ at the nipple tip in $r=0$ which is such that

$$\mathscr{R}_-(t) = 2\,(\nabla^2\xi(0,t))^{-1} = \frac{1}{k_m^2\xi(0,t)} \sim \mathrm{e}^{-\sigma t} \tag{4.17}$$

is expected to decay as the inverse the nipple amplitude $\xi(0,t)$, with the same rate σ, as seen in figure 4.

At the end of the exponential stage of the instability, this radius of curvature decays abruptly, and remains afterwards constant. The saturated shape of the nipple is such that the Laplace pressure $2\gamma/\mathscr{R}_-$ equilibrates the hydrostatic pressure $\rho g\beta/(1-\beta)\mathscr{R}_-$ where $\mathscr{R}_-$ is now the constant radius of curvature at the nipple tip thus given by

$$\mathscr{R}_- = \sqrt{\frac{1-\beta}{\beta}\frac{2\gamma}{\rho g}} \tag{4.18}$$

and appears as the capillary length of the problem. Experiments using two different liquids are quantitatively consistent with (4.18), as shown in figure 4.

5. Discussion

With the help of a simple experiment, we have shown that the acceleration of the free surface of a falling liquid can be larger than the acceleration of gravity. Super acceleration of the upper interface of a liquid volume falling in a weakly expanding tube comes from the additional positive pressure gradient induced by the geometry which adds to the gravity body force. A perturbative expansion of the base Euler solution further accounts for the interface shape, and stability. In particular, the positive pressure gradient at the interface makes it unstable, forming a concentrated 'nipple' on top of the essentially flat base solution. Note that the 'principle of equivalence' stating that no physical phenomenon can put in evidence

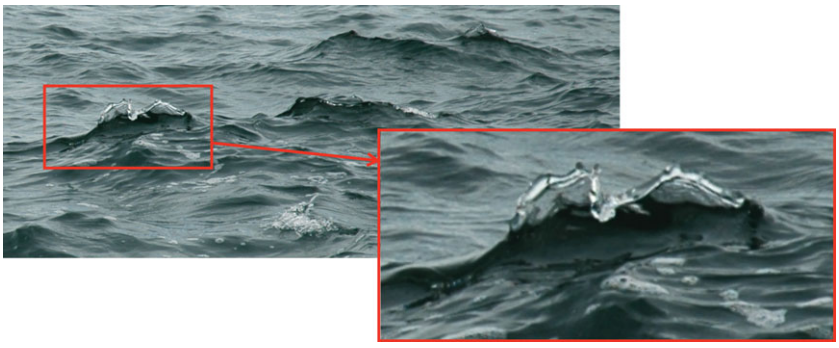

FIGURE 5. Pointed wave crests on the sea shore in Marseilles. One of them breaks.

a system in free fall, does not apply here: the added (or subtracted) acceleration becomes a non-zero acceleration in the free falling frame.

It makes sense at this stage to worry about the relevance of our model to wave-breaking. Vertical acceleration has been identified long ago as possibly responsible for (or concommitent with) the phenomenon (see e.g. Penney & Price 1952; Phillips 1958). Our geometry, constrained by solid walls obviously brings us away from the real situation. The positive pressure gradient $\partial_z p$ 'sucking' downwards the interface is a consequence of this geometrical confinement, which does not seem to have an equivalent in free surface flows. In a wave problem in the infinite depth limit, the boundary condition for the pressure is imposed at $z \to -\infty$. In this respect the pressure, at least for an immobile fluid at $t = 0$ (i.e. without contributions from the Reynolds stress $u_i \partial_i u_j$ to the pressure), is a harmonic function tending to $-gz$ at large $(-z)$, and equal to 0 on the free upper surface. Consider now the following problem: given the shape of the free surface, and that the fluid velocity is exactly zero at $t = 0$, is it possible to have somewhere on the free surface a downward acceleration greater than g ? The answer seems to be no, precisely because the iso-pressure surfaces draw a set of surfaces that are quasi parallel to the interface. Therefore, without resorting to Reynolds stresses, the hydrostatic pressure can only grow away from the free surface. However, wave-breaking does occur with standing waves (Taylor 1953), and in Nature, doing so in a fashion very similar to that in our experiment, as figure 5 illustrates: a 'nipple' forms at the falling wave crest, bends, and soon splashes on the sea surface, forming foam and spume. Is the present study definitely irrelevant to that common but yet unexplained phenomenon ?

The present experiments and analysis have been made five years ago. In the meantime, we have enjoyed discussions with A. Antkowiak, B. Audoly and S. Le Dizés.

REFERENCES

BERNOULLI, D. 1738 *Hydrodynamica*. Strasbourg.

CALKIN, M. G. & MARCH, R. H. 1989 The dynamics of a free falling chain: I. *Am. J. Phys.* **57** (2), 154–157.

CLAVIN, P. & WILLIAMS, F. 2005 Asymptotic spike evolution in Rayleigh–Taylor instability. *J. Fluid Mech.* **525**, 105–113.

DUCHEMIN, L. 2008 Self-focusing of thin liquid jets. *Proc. R. Soc.* A **464**, 197–206.

HIRATA, K. & CRAIK, A. D. D. 2003 Nonlinear oscillations in three-armed tubes. *Eur. J. Mech.* B – *Fluids* **22**, 3–26.

Newton, I. 1687 *Principia Mathematica*. London.

Paterson, A. R. 1983 *A First Course in Fluid Dynamics*. Cambridge University Press.

Penney, W. G. & Price, A. T. 1952 Finite periodic stationary gravity waves in a perfect liquid. *Phil. Trans. R. Soc.* A **244**, 254–284.

Phillips, O. M. 1958 The equilibrium range in the spectrum of wind-generated waves. *J. Fluid Mech.* **4** (4), 426–434.

Schager, M., Steindl, A. & Troger, H. 1997 On the paradox of the free falling folded chain. *Acta Mech.* **125**, 155–168.

Taylor, G. I. 1953 An experimental study of standing waves. *Proc. R. Soc.* A **CCXVIII**, 44–59.